Recent Advances in Ultra-High-Temperature Ceramic Coatings for Various Applications

K. Deepthi Jayan

Abstract In the past, the research on high-temperature applications of materials has focussed mainly on SiC and Si_3N_4 only. The recent advances in propulsion and hypersonic concepts and the related applications have resulted in the search for new categories of materials capable of withstanding very high temperature. The borides, nitrides and carbides of various transition metals can be employed for synthesising ultra-high-temperature ceramic (UHTC) coatings. These materials possess excessively huge melting point along with substantial mechanical properties at extreme temperature, making them suitable for several high-temperature structural and other environmental applications such as in rockets, hypersonic vehicles and engine components. The inherent brittleness as well as extremely feeble shock resistance of ceramic materials can be overcome to a greater extent with the application of ultra-high-temperature ceramic coatings and fibre-reinforced ultra-high-temperature ceramic materials. UHTC coatings are extremely useful as thermal shock absorbers, surface seals and leak minimisers. The carbothermal reduction method is the oldest method employed for the synthesis of UHTCs. However, many other solid-state powders-based and solution-based methods have been employed recently to enhance the unique properties of them. The synthesis methods face a few challenges and require highly refined approaches to synthesis high purity UHTC powders, suitable chemical synthesis reactions and proper selection of precursors delivering excellent chemical yield and less degradation. The microstructural aspects of the synthesised UHTCs can be identified through suitable characterisation techniques including in situ characterisation. Apart from the excellent mechanical properties like excellent elasticity, flexural strength, and fracture toughness, UHTCs must be assessed for its machinability when they are employed for hypersonic and space applications. The thermodynamic properties such as the coefficient of thermal expansion, thermal conductivity and total hemispherical conductivity play a significant role in determining the high-temperature applications of UHTCs. Oxidation resistance at high-temperature environment is the most wanted property of materials especially when

K. D. Jayan (✉)
Department of Basic Sciences and Humanities, Rajagiri School of Engineering and Technology (Autonomous), Rajagiri Valley, Kakkanad, Kochi, Kerala 682039, India
e-mail: deepthij@rajagiritech.edu.in

A. Pakseresht and K. K. Amirtharaj Mosas (eds.), *Ceramic Coatings for High-Temperature Environments*, Engineering Materials,
https://doi.org/10.1007/978-3-031-40809-0_13

they are employed for various space applications. Recent advances show that the use of multilayers of the high-temperature ceramic protective coating reduces oxidation of carbon–carbon (C–C) composite materials and protect them from aerothermal heating at temperatures above 3273 K. Hence, the mechanisms, kinetics and the end products of oxidation mechanisms help the researchers to identify the strengths and weaknesses of the UHTCs when employed for specific applications. This chapter focusses mainly on the recent advances in the synthesis and characterisation techniques of UHTCs giving due importance to their various properties and oxidation mechanisms. The atomistic computational modelling and simulation studies on the impacts of defects on the thermal and mechanical properties of UHTCs are found to be extremely useful to identify their drawbacks prior to their employment in various device configurations. In a similar way, the computational studies on UHTCs by employing thermal shock modelling tools provide useful information about their thermal shock resistance. This chapter also provides a brief overview of the applications of UHTCs along with a description of the properties and applications of the emerging high entropy UHTCs.

Keywords Ultra-high-temperature composites · Sintering · Simulation · High entropy materials

1 Introduction

Both the preservation of existing natural resources and their optimal and cost-effective utilisation in the design and manufacture of all high-temperature equipment are the guiding concerns behind the selection of materials today. In account of these considerations, scientists have concentrated on enhancing energy production efficiency of the equipment while concurrently reducing hazardous emissions, primarily CO_2 and NO_x, from them through a wise selection of raw materials [1]. One way to achieve this is to keep the engines and turbines at high temperature with a simultaneous reduction in the size and weight of its components, thereby creating a high-temperature environment with no cooling system in its vicinity. This will result in the development of ultra-high thrust resulting from a reduced fuel utilisation leading to a reduction in the emission of toxic gases. In the past, the research on high-temperature applications of materials has focussed mainly on super alloys such as SiC and Si_3N_4 only. However, these alloys possess some disadvantages under such operating environments and hence require the best materials including ceramic materials and composites, for such applications. In the quest for identifying suitable materials for high-temperature applications, researchers have tried several transition metals and their derivatives. The study shows that carbides, nitrides, as well as borides of transition metals can be employed as a suitable material for high-temperature applications [2, 3]. The ceramic metal composites (CMCs), thermal and environmental barrier coatings, etc., can be employed in high-temperature applications for various industries. These coatings when employed in fuel cells improve the efficiency of power generation while keeping the emission of toxic gases to a lower level. The solid oxide fuel cells composed of ceramic metal composites can operate with the help of the fuels such as hydrogen or light hydrocarbons at high-temperature range, still maintaining a low rate of performance degradation and generating ultraclean energy.

Currently, above 3000 materials that possess high melting points, generally above 2273 K, including the popularly used high-temperature material, SiC exists [4]. The other high-temperature materials of interest include refractory metals, viz. Hf, Ir, Nb, etc., oxides of Hf, U, Th, Zr and a wide group of borides, carbides and nitrides of transition metals and their composites. Refractory diboride compounds possess excellent oxidation resistance and hence the group IV and V element-based refractory diboride materials have gained research focus. Among these materials, the diborides of Hf and Zr form the most potential candidates in ultra-high-temperature application fields [5, 6]. The high melting point and the hardness of these metals arise from the strong covalent bonding between the constituent elements of the material. They also possess a high negative free energy of formation, which accounts for the good thermal and chemical stability of the diboride compounds. The high thermal shock resistance of these diboride compounds arises from their excellent thermal conductivity and hence they can be employed for various high-temperature applications. In a similar way, non-oxide ceramic matrix composites (CMCs) formed of carbon or SiC fibres-reinforced SiC-based materials find significant importance in high-temperature applications owing to their excellent thermal conductivity, high thermal shock stability, creep, oxidation and wear resistance along with enhanced toughness compared to the monolithic material. When employed for high-temperature applications, the fibre-matrix interface in non-oxide CMCs controls the fracture toughness of material thereby hinders its transversal fracture via deflections of cracks present initially in the structure [7].

The study on UHTCs started in the late 1800s, however, technologies based on UHTCs have emerged during the 1950s only, with the increasing interest in developing new space technologies that can withstand high-temperature conditions. The research interest in UHTCs has further enhanced with the development of aerospace applications such as rocket motors, hypersonic aerospace vehicles and scramjet propulsion [8]. One of the difficulties faced during aerospace applications include the production of very high-temperature above 2000 °C at the sharp leading edges and control surfaces when the device is operated at hypersonic speeds, thus leading to heat flux and the emission of reactive gas species. Such applications employ diboride-based UHTCs due to their excellent thermal conductivity, mechanical strength and oxidation resistance, while dicarbide and dinitride-based UHTCs can be employed for the device components such as nozzle throats, divert/attitude control thrusters and nozzle liners that need to withstand heavy loads and hence require excellent mechanical strength [9, 10]. Despite the advances in the knowledge of several factors related to UHTCs such as the synthesis, processing, thermochemical properties and oxidation, a few key challenges in the understandings of UHTCs do prevail. This chapter focusses on the advances that occurred in the research of various UHTC materials and their applications in various fields.

2 New UHTC Material Systems

A wide utilisation of the UHTCs for very high-temperature applications necessitates the need for the availability of a broad category of materials capable of exhibiting excellent thermodynamic properties at high temperature. The UHTC materials usually are formed by developing a strong covalent bond between the early transition elements and carbon, nitrogen or boron. The strong covalent bond is responsible for the ultra-hardness, stiffness and melting point of these compounds. These materials also possess certain degree of metallic bond character and is responsible for their high thermal and electrical conductivities in comparison with other oxide materials. Such a combination of metal like and ceramic like properties enable them to overcome extreme temperature, mechanical loads, heat flux and radiation levels. Figure 1 shows a comparison of the melting point and the density of various boride, carbide or nitride-based UHTCs that have prominent applications in various fields at high temperature [11]. The subsequent subsections discuss the properties and applications of various types of UHTCs that are carbides, nitrides or borides of early transition metals.

2.1 Boride-Based UHTCs

Recent advances in the field of aerodynamics and propulsion systems indicate the requirement of next generation aircrafts with speeds exceeding the speed of modern supersonic aircrafts, which in turn necessitates the inclusion of thin and sharp leading-edge profiles that enhances the manoeuvrability, safety and the performance of the

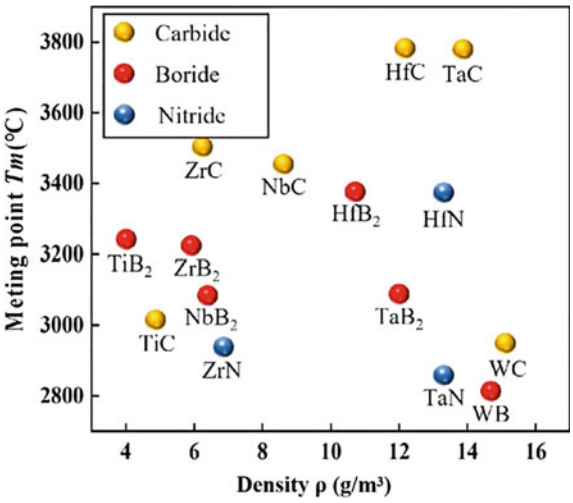

Fig. 1 Plot indicating the melting point of various UHTCs as a function of its density [11]. Copyright 2021. Reproduced with permission from MDPI

aircrafts while reducing the drag experienced during its operation. Transfer of fractional energy to the surface and the resulting concentration at the stagnation points of the leading edges of the aircraft occurs when the flight speed exceeds 5 Mach. At high speeds, chemical heating occurs due to the dissociation of oxygen and nitrogen in air and their subsequent recombination at the surface. These factors contribute to a very high surface temperature above 2273 K at the leading-edge region of the aircraft [6]. The melting point of conventional aircraft materials is well below this temperature and hence may result in the damage of the aircraft when operated under high operating temperature conditions. This can be avoided by the deposition of temperature resistant and highly conductive coating materials on the surface of the leading-edge region of the aircraft. Such coating materials are made up of a combination of materials that possess high thermal conductivity and high melting temperatures, so as to withstand the extremely high-temperature environments and to dissipate the heat from the thinner leading edge of the aircraft to other thicker regions without damaging the environment. In this regard, the boride-based ultra-high-temperature coating materials are extremely useful which in turn can protect the environment also [12, 13].

The refractory metal diborides of Zr and Hf are excellent thermal protection system (TPS) coating materials that possess excellent thermal conductivity and high melting points. The melting temperature of ZrB_2 and HfB_2 is 3523 K and 3653 K, respectively. ZrB_2 and HfB_2 possess a thermal conductivity of 60 W/m K and 100 W/m K, respectively. These materials also possess excellent mechanical and elastic properties along with corrosion and wear resistance and chemical stability. A group of researchers have developed a high strength zirconium diboride-based ceramic material by employing hot-pressing technique. They have developed ZrB_2 by incorporating 10, 20 and 30 vol% of SiC particulate materials in the powder form [14]. To measure the mechanical strength of the material, the four-points bend strength, fracture strength, various elastic constants, elastic modulus as well as hardness have been estimated. The mechanical strength and the hardness of the ZrB_2 material was improved with the addition of SiC. The addition of 20 to 30 vol% of SiC has improved the strength of the ZrB_2 to 1000 MPa, while the material in the absence of SiC provided a mechanical strength of 565 MPa only. It was identified that the improvement in the strength of the material is due to the increase in the grain size of the material. Another study employed a number of Hf-based carbides and W-based materials in combination with SiC and HfC to improve the oxidation [15]. Oxidation tests were performed on HfB_2-SiC, HfB_2-HfC, HfB_2–WC–SiC and HfB_2–WSi_2 ceramics with the help of oxyacetylene torch by oxidising the samples between 2373 and 2573 K. Another study focussed on estimating the thermal conductivity of HfB_2-based UHTC material by employing laser flash diffusivity studies in the temperature range of 298 K to 873 K. A 20 vol% SiC was added to the commercially available HfB_2 to prepare the HfB_2-SiC composites. Conventional hot pressing or spark plasma sintering was employed to consolidate the samples. The differences in processing result in changes with magnitude of thermal conductivity and its dependence on temperature. A network model of effective thermal conductivity has been developed by including the influences of porosity, grain size, Kapitza resistance and individual thermal conductivities.

The strength and oxidation resistance of diboride UHTCs can be enhanced further by combining it with other refractory metals such as SiC or $MoSi_2$. The application of hot pressing at a temperature above 2273 K results in borides and boride-based particulate composites. The addition of C, B_4C and $MoSi_2$ to the boride materials via pressureless sintering methods results in the development of near net-shaped diboride ceramics. The flexure strengths of HfB_2 and ZrB_2 ceramics at room temperature are typically in the range of 300 MPa to 500 MPa. The flexure strengths can be improved to 800 MPa to 1000 MPa with the application of additives such as a trace concentration of SiC or $MoSi_2$ [14]. A major concern with boride ceramic materials is the retention of strength at high temperatures. When the temperature reaches 1273 K, the strength of fine-grained ceramics that contain particulate reinforcements tend to increase by a small amount [16]. However, when the temperature reaches 1473 K, the strength of the material decreases by 50%. A study on HfB_2 indicated a strength retention at temperature as high as 1773 K, via spark plasma sintering process [17].

2.2 Carbide-Based UHTCs

The research on carbide ceramic materials has been limited due to their high cost and the need for sophisticated equipment and technique for their preparation. Due to the abundance of Ti-based carbides in earth crust, the most studies carbide ceramic material is TiC. The high melting point, low density, excellent thermal conductivity and ultra-high hardness of TiC ceramic material make it suitable for high-temperature applications. TiC can also act as a thermal protection material for aircraft applications [18–20]. The ideal and defect crystal structure of TiC material is shown in Fig. 2. The study performed by Mao et al. demonstrated that hardness of TiC ceramic material can be enhanced by increasing the C content in the compound [11]. The Zr-based UHTC composites possess supreme mechanical and physical characteristics including high electrical and thermal conductivity, hardness, mechanical strength, etc. Though ZrC is cheap and abundant, the issues associated with sintering and the moderate value of fracture toughness of the material hinder it from wide spread applications at high temperature. However, the ZrC materials can be further toughened by reinforcing it with fibres, graphene flakes and layered structures, etc. [21].

A recent study on the optical properties of boride- and carbide-based UHTC materials indicates that adding SiC to the materials enhanced the solar energy absorption properties of them. The study focussed on estimating the optical properties of a few materials such as diborides of Hf and carbides of Hf, HfB_2–SiC and HfB_2–HfC–SiC. The above-mentioned materials were synthesised via spark plasma sintering method from ceramic powders. The synthesised materials exhibited a relative density of 95% that arises from the addition of SiC to the material, which in turn helps in improving the oxidation resistance of composites [22]. The ZrB_2 as well as HfB_2 materials are considered as potential candidates for high-temperature uses as they possess

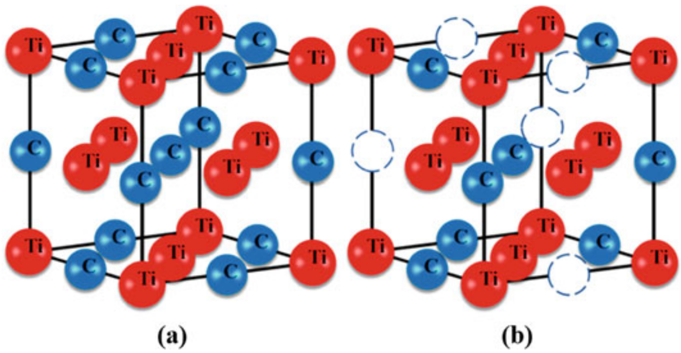

Fig. 2 **a** Ideal crystal structure and **b** defect crystal structure of TiC [11]. Copyright 2021. Reproduced with permission from MDPI

excellent oxidation resistance at an extreme temperature of 1773 K. However, rapid evaporation of boron oxides at high-temperature results in the loss of material and the monolithic ZrB_2 fails to its low thermal shock resistance and poor toughness when employed for high-temperature applications [23, 24]. A mixed boride- and carbide-based composite UHTC, $Zr_{0.8}Ti_{0.2}C_{0.74}B_{0.26}$ showed that it possesses excellent ablation resistance in the temperature range 2273 K to 3273 K when compared to the conventional ZrC-based UHTCs [25]. The composite was prepared by reactive melt infiltration and pack cementation and is identified as suitable for hypersonic vehicles, rockets and other defence systems.

Among various potential candidates for UHTCs, the ternary $Ta_xHf_{1-x}C$ $(0 < x < 1)$ ceramics have attracted great attention owing to their ultra-high melting temperature above 3973 K. The simple crystal structure of these ternary ceramic compounds resembles the Fm3m space group of NaCl, which in turn helps in the generation of a continuous solid solution of $Ta_xHf_{1-x}C$ $(0 < x < 1)$ with TaC and HfC in all possible compositional ranges. The ablation resistance of materials is a significant parameter that determines its suitability for high-temperature deployment as is determined by the melting point and integrity of oxide scale exposed to extreme scouting of heat fluxes. In a study, a group of researchers estimated the ablation resistance of $Ta_{0.8}Hf_{0.2}C$ and $Ta_{0.8}Hf_{0.2}C$-10 vol% SiC ceramics via a plasma flame test in air. A 20 μm thick unstable single oxide layer of monolithic $Ta_{0.8}Hf_{0.2}C$ was detected on the completion of ablation test, while a more stable double reaction layer was identified for the $Ta_{0.8}Hf_{0.2}C$-10 vol% SiC ceramic on the completion of ablation [26].

2.3 Nitride-Based UHTCs

Nitride-based UHTCs are generally employed for industrial applications such as hard coatings, diffusion barriers, heat mirrors and decorative coatings. The UHTC material, ZrN, can be employed as an IR reflective material. ZrN undergoes oxidation at room temperature and hence requires densification via pressureless sintering, hot pressing or hot isostatic pressing. However, these methods require a high temperature of 2273 K, along with high applied loads due to the high melting point of the material, strong covalent bonding and the presence of ZrO_2 oxide layer in the powder surface [27, 28]. Selective laser reaction sintering (SLRS) method can be employed for manufacturing nearly net-shaped UHTC materials including HfN, ZrN and TiN along with carbides and borides of transition metal elements. The group IV transition metals and their oxides are chemically transformed and incorporated into very thin layers of UHTCs via the selective laser interaction sintering in presence of 100% vol of CH_4 or NH_3 gas. The SLRS processing of transition metals and their oxides resulted in the development of near stoichiometric single phases of UHTCs [29].

In a study, a group of researchers synthesised non-stoichiometric hafnium carbonitrides (HfC_xN_y) by employing a short-term high-energy ball milling of Hf and C powders. This was followed by the combustion of Hf/C composite particles in a nitrogen environment at a pressure of 0.8 MPa. The synthesised composite material exhibited a high melting point much greater than that for HfC. The non-stoichiometric hafnium carbonitride thus developed further processed to bulk ceramic material via spark plasma sintering. The bulk composite exhibited a relative density of 98%, along with excellent fracture toughness and hardness [30]. Due to the beneficial properties and application suitability of boride- and carbide-based UHTCs, not much research studies have been done so far on the nitride-based UHTCs, and the field of nitride-based UHTCs is still developing at a great pace.

3 Synthesis Techniques of UHTCs

The boride- and carbide-based UHTCs can be employed for a number of applications including the coating for re-entry vehicles in space applications. Such applications require high-quality coating materials with sufficient hardness and mechanical strength along with high heat conductivity [31]. There are a number of preparation methods available for the development of UHTCs. Depending on the type of application for which UHTCs are employed, a specific preparation method may be employed. The following subsections discuss the various synthesis techniques employed for the preparation of UHTCs.

3.1 Powder Synthesis Method

In certain applications, the purity of UHTC composite powder employed must be high for ensuring the desired properties and microstructures for the synthesised UHTC materials. The powder synthesis method is a suitable method for applications that require the synthesis of diborides of Zr and Hf. It includes the synthesis from the reaction between elements, borothermic or carbothermic or metallothermic reduction of metal oxides, boron carbide reduction of metal oxides in carbon rich environment, molten salt electrolysis, solution-based methods and synthesis from polymer precursors.

3.1.1 Synthesis of UHTCs from Elements

The simplest method for the production of boride powder includes the chemical reaction between boron and powdered metals and thereby establishing a control over the stoichiometry of the boride powder [32]. The densification of the generated ZrB_2 or HfB_2 can be done by plasma sintering method or hot-pressing method. A method known as self-propagating high-temperature synthesis (SHS) that utilises the high exothermic energy of reactions in developing a high-temperature environment necessary for completion of chemical reactions between the boron and metal can also be employed for the synthesis of diboride-based UHTCs. Low-cost equipment requirement, low energy consumption, short process time and excellent purity are some of the benefits of employing this method. However, the retention of more than 50% of porosity along with incompletion of chemical reactions due to fast heating is some drawbacks of this method [33].

3.1.2 Borothermic Reduction of Metal Oxide

Borothermic reduction of metal oxides at a temperature above 1273 K leads to the development of pure boride materials. A drawback of this method is the wastage of boron via the formation of boron oxide and hence is not deployed for industrial applications. This is evident from reduction in boron content of product thus prepared. By introducing mechanical milling, it is possible to lower the reaction temperature, enhance the mixing of chemicals via reduction of grain size and introduces lattice deformations leading to faster diffusion and mass transfer rates [34].

3.1.3 Carbothermic Reduction of Metal Oxide

Carbothermic reduction of metal oxide and boron oxide (B_2O_3) is an easy and simple method for the formation of boride materials at a high temperature of 2073 K [35]. A non-stoichiometric compound is formed via carbothermal reduction of the metal oxide and leads to a loss of B_2O_3 during the reduction process and the deposition of residual carbon. The same method can be employed for the formation of boride whiskers. Nickel or cobalt can act as a catalyst during the process, however, nickel acts as a better catalyst during the process that also results in the formation of defects necessary for heat and mass transfer.

3.1.4 Boron Carbide Reduction of Metal Oxide

Here, powdered boride can be prepared at a temperature above 2073 K and keeping time for more than one hour, by the following reaction:

$$MO_2 + \frac{1}{2}B_4C + \frac{3}{2}C \rightarrow MB_2 + 4CO \quad \text{where } M = \text{Zr or Hf}$$

This reaction results in wastage of boron from boride powder and leads to the development of residual carbon and non-stoichiometric boride. The presence of unwanted oxygen can be removed by employing high vacuum during the reduction process.

The synthesis of boride is followed by its densification, which may be affected by the variation in size of the particle with the synthesis temperature. The synthesis stability and particle size are inversely related to the synthesis temperature [36].

3.1.5 Metallothermic Reduction

The metallothermic reduction can produce boride powder by employing the following the chemical reaction with magnesium as the reducing agent.

$$MO_2 + B_2O_3 + 5Mg \rightarrow MB_2 + 5MgO \quad \text{where } M = \text{Zr or Hf}$$

In metallothermic reduction, magnesium is employed as the reducing agent because of the ability of the formed MgO to leach out from the material, thus forming a pure boride phase. This reaction route also employs mechanical alloying to reduce the reaction temperature. Since it is an exothermic process, it can employ the SHS process. The sudden cooling and heating process via SHS generates a number of defects in the material and enhances the mass transfer rate. In order to overcome the incomplete reaction via SHS arising during the production of ZrB_2 from ZrO_2, Mg and H_3BO_3, a double SHS (DSHS) is generally performed, in which product of the first SHS reaction is mixed to Mg and H_3BO_3 and then a second SHS is performed on the mixture, thereby enhancing conversion process [37].

3.1.6 Solution-Based Techniques

Solution-based techniques can be employed for the synthesis of fine powders of borides, carbides and nitrides of transition metals due to the close contact between the reactants. At a low temperature of 1773 K, a group of researchers have prepared ZrB_2 powder employing hybrid precursor made of zirconium oxychloride ($ZrOCl_2$ $0.8H_2O$), boric acid and phenolic resin which provide zirconia, boron oxide and carbon, respectively. The ZrB_2 powder thus synthesised is found to contain larger surface area and lower oxygen content in comparison with the surface area and oxygen content of commercially available ZrB_2 powder [38].

3.1.7 Molten Salt Electrolysis

Molten salt electrolysis method is employed for the preparation of diverse metal borides. One such metal boride, namely ZrB_2 can be deposited on nickel cathode from a mixture of ZrO_2 as well as B_2O_3 by dissolving with molten Na_3AlF_6 at 1293 K. The anode was prepared from graphite crucible. ZrB_2 deposit was found to be dendritic as well as fully non-adherent. A study tried to develop ZrB_2 on a Ni cathode from cryolite-alumina melts that contains Zr and B_2O_3 [39].

3.1.8 Synthesis by Polymer Precursor Route

A processible polymeric precursor for the preparation of boride materials can be developed via thoroughly dispersing a metal oxide in boron carbide polymeric precursor. This mixture with an increase of temperature will lead to formation of boron carbide as well as carbon, which is assisted subsequently by a chemical reaction to develop boride or a direct chemical reaction of a metal oxide with a polymer to form the final boride product [40].

3.2 Sol–Gel Method

Sol–gel method can be employed for the synthesis of diverse forms of UHTCs. It involves many steps including the mixing of chemicals in a solution followed by the gelation, drying and a post-treatment to get the final UHTC product. In this method, a homogeneous liquid state is employed initially that results in the development of nanopowders, fibres, thin films or porous monoliths of UHTCs with refined microstructures and mechanical properties. There are three commonly employed sol–gel methods for the synthesis of UHTCs as depicted in Fig. 3. In the templating method, infiltration or impregnation of the porous template is done with the preceramic sol, followed by drying the green body and heating it up to 1873 K for the development of porous UHTCs by means of a reduction reaction. The template

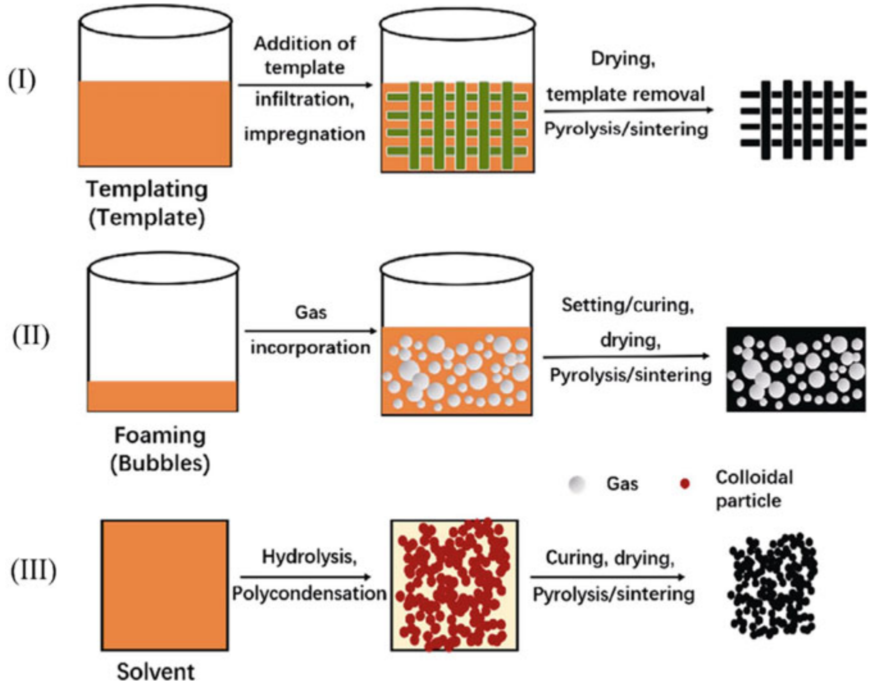

Fig. 3 Schematic representation of sol–gel process employed for the synthesis of porous UHTCs [41]. Copyright 2020. Reproduced with permission from SpringerLink

is later removed to form a stand-alone porous UHTC. The porous UHTC exhibits the same morphology as that of the original porous template, and however, undergoes shrinking during the process. In the second sol–gel method known as foaming, bubbles are developed initially with the help of air or any other volatile agents into the preceramic sol and results in green body after leaving it for setting. The third method, known as solvent evaporation, is a template free method, in which a preceramic sol–gel is transformed to a preceramic wet gel. The solvent is then evaporated to form porous UHTCs at the end [41].

4 Densification Methods for UHTCs

The poor intrinsic self-diffusion properties, strong covalent bonding and the extremely high melting points prevent the densification of UHTCs, which is required for the further employment of these materials in diverse applications. The UHTC surfaces get covered with metal oxides and it prevents the contact between boride particles, which in turn adversely affects the densification process. At high temperature, an excess growth of grains occur that leads to poor mechanical properties.

Densification process of UHTCs can be performed only at extreme pressure and temperature conditions. Some important densification processes include pressureless sintering, hot pressing, spark plasma sintering, microwave sintering and laser-assisted sintering. The following subsections briefly describe these methods employed for the densification of various types of UHTCs.

4.1 Pressureless Sintering

Ceramic materials with very dense shape can be prepared by means of pressureless sintering techniques. In the method, a cold isostatic pressing may be applied to prepare green compacts with excellent strength and then green pellets are fired in an induction furnace at a particular temperature under a controlled experimental environment. This method can be employed to produce near finished UHTCs, that do not require any additional finishing techniques such as diamond machining. One drawback of pressureless sintering is that the properties of the UHTCs developed are much inferior to that developed by means of other types of densification techniques. This arises due to the dominant nature of evaporation–condensation mechanisms during this process. Diverse additives have been added during the densification process to form boride-based UHTCs. It is also possible to add metals, carbides and silicides to improve the process of densification. Adding carbon and carbides help in the densification of borides to a high relative density of 95% at a high temperature of 2273 K. The interaction of additives with the surface oxide layer leads to the enhancement of surface energy, which in turn leads to the enhancement in densification. This method can be employed for the generation of UHTCs which do not require a high-density value. The porosity of the material results in lowering the stiffness of the material and thereby its thermal conductivity also. In a study, the pressureless sintering technique was employed by a group of researchers for the fabrication of a UHTC composite material ZrB_2–SiC at a high temperature of 2273 K to 2473 K for 1 h in an argon environment. The composite was found to exhibit a relative density of 98.12% and a hardness of 15.02 GPa at 2473 K [42]. In a recent study, a ZrB_2–SiC–Cr_xC_y, ZrB_2–SiC–Mo_xC_y, ZrB_2–CrC, ZrB_2–MoC as well as ZrB_2–WC composites were densified via a pressureless sintering method. As per the study, WC exhibited the highest ability to densify ZrB_2 and ZrB_2–SiC, while Cr_3C_2 exhibited the lowest ability to densify them [43].

4.2 Reactive Sintering

UHTCs formed of the composites ZrB_2–SiC are employed for extreme high-temperature applications, wherein the temperature exceeds 2273 K. The oxidation resistant nature of UHTCs revealed various methods for enhancing the oxidation performance that include the control of powders used at the beginning of the process, composition of the initial materials and size distribution, type of additives, mixing of these materials and the densification methods employed. This helps in improving the viscosity of the liquid phases developed at high temperature. The addition of SiC is suitable for low temperature densification while La addition leads to the formation of ZrO_2 via liquid phase sintering. These methods result in the generation of self-generating refractory oxidation barriers, which are of superior importance in the field of high-temperature coating materials.

In this regard, the pressureless reactive sintering provides high purity products at low processing temperature and time and results in modifying grain boundary of materials. A green body having a lower porosity produces a product with high density. This process generates defects and dislocations via shock consolidation process, leading to diffusivity, which in turn enhances the density and thermal conductivity of the material. In a study, a group of researchers have employed a selective laser reaction sintering (SLRS) to prepare net-shaped UHTCs including HfC, ZrC, HfN, ZrN and TiN. The method was able to produce near stoichiometric UHTCs, however, some volumetric changes were observed due to gas–solid reactivity in the case of single component precursors. The volume changes of the metal or metal oxide precursors were compensated by the inclusion of composite metal/metal oxide precursors, which induces conversion induced stresses [44].

4.3 Hot Pressing

Dense UHTCs can be synthesised by means of hot-pressing method as the pressureless sintering of UHTCs in the absence of additives is a complicated process. Hot-pressing method employs an extremely high pressure and temperature to a powder compact. On applying pressure, diffusion of particles at the contact points occurs, which in turn is affected by the particle size. A ball milling is employed to generate UHTC powder with a size of 2 μm approximately before the employment of hot-pressing method. The powder obtained after milling is enriched with graphite die, which is subsequently subjected to high temperature in an argon rich environment. A UHTC composite ZrB_2–HfC–C_f was developed by employing a low temperature hot-pressing method using nanosized ZrB_2 powder. The composite material was found to exhibit non-brittleness, excellent work of fracture and a comparatively high thermal shock resistance. The material also exhibited excellent oxidation resistance, which is required for high-temperature applications [45].

4.4 Reactive Hot Pressing

This represents a technique of densification, wherein the reaction proceeds at a slow pace via the diffusion of solid-state particles. In this method, thermodynamically favourable reactions occur in a completely controlled manner that ensures the perfect conversion of reactants to products. This reaction proceeds via simultaneous application of pressure that ensures the formation of dense bodies of UHTCs. This also eliminates the need for further powder processing of the densified UHTC. With the help of Si, Hf and B_4C as the precursors, a HfB_2–SiC UHTC composite was synthesised by employing a reactive hot-pressing method for its densification. The reduction in size of precursors was tested by employing a vibration milling and was identified as a critical parameter that determines the microstructure of the UHTCs. The vibration milled sample exhibited a uniform oxidation, while the bare sample exhibited non-uniform oxidation. The mechanical properties of the material were tested and it was identified that the reduction in size of the precursors via vibration milling leads to an increased flexural strength also [46].

4.5 Spark Plasma Sintering

It is an advanced method for the densification of UHTCs, wherein it is possible to develop high-density UHTCs at a low reaction temperature during a very short span of time. A pulsed direct current is allowed to flow through the graphite plungers and dies along with the applications of pressure. The schematic representation of a SPS is shown in Fig. 4. This method is alternatively called as field-assisted sintering technique (FAST). It consists of a mechanical loading system, which can also act as a high-power electrical circuit kept in a controlled experimental condition. The simultaneous applications of current and pressure result in the densification of the UHTC [47]. SPS can be employed for homogeneous distribution of whiskers in UHTC composites. In a work, a group of researchers have employed SPS to densify a UHTC composite composed of B_4C and SiC_w powder mixtures. The method employed the densification of B_4C–SiCw composite by using various wt% of SiC approximately ranging up to 12 wt% of the composite at a high temperature of 2073 K for a duration of 10 min at 50 MPa pressure. The study showed that the B_4C–SiCw formed with a 9 wt% of SiC provided excellent Vicker's hardness, flexural strength and fracture toughness [48].

4.6 Microwave Sintering

Microwave sintering is a method employed for densifying UHTCs, in which heating of powder compact is attained via the application of microwaves to sample. Some materials do not possess the ability to absorb microwaves at room temperature; however, they can absorb microwaves if some microwave absorbing second phase is added. This technique involves a uniform and rapid heating of the sample since the microwave energy is directly given to the specimen without conducting it to the specimen. In a study, Ni was employed as a second microwave absorbing phase for

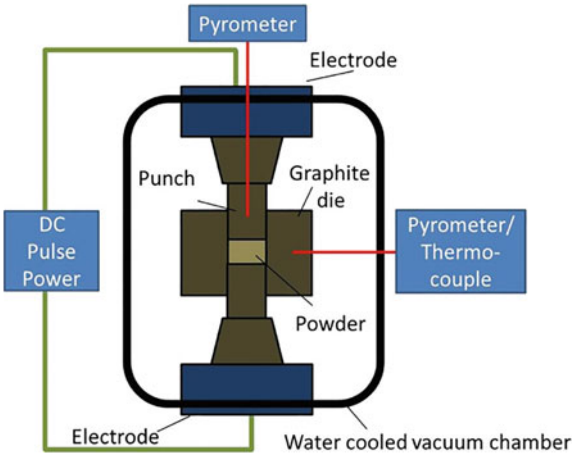

Fig. 4 Schematic representation of a SPS employed for the densification of UHTCs [47]. Copyright 2014. Reproduced with permission from Wiley online library

the densification of TiC. The study showed that density of microwave sintered specimen is 8–10% above that densified by means of conventional sintering techniques [49]. Another study employed microwave sintering method for the densification of ZrB_2-SiC composite and investigated its mechanical and other metallurgical characteristics. The study showed the highest relative density and Vickers hardness values of 97.72% and 17.03 GPa, respectively, for ZrB_2–25 vol% SiC composite [50].

4.7 Laser Sintering

This method produces dense material by sintering the powder layer by layer with the help of laser. The sample in the power form is irradiated with a laser beam, resulting in a rise in temperature of sample leading to a size increment for the grain and eventually densification of sample. This method ensures high purity sample densification due to minimum contact between the particles. A group of researchers have developed a ZrB_2 UHTC with uniform surface morphology via laser sintering technique. The laser sintering also employs rapid cooling and leads in developing needle like nanostructures on material surface [51].

5 Coating Methods

Certain applications require UHTCs in coating form, which can be achieved by diverse methods. However, not all coating methods are applicable for UHTCs composed of borides of Zr and Hf. Vapour deposition process is the most suitable method for the development of refractory UHTCs. Some useful coating methods such as chemical vapour deposition, physical vapour deposition and plasma spray that are employed for the coating of refractory borides are briefly described in the following subsections.

5.1 Chemical Vapour Deposition (CVD) Method

The chemical reaction of reactant vapours on a substrate results in the development of UHTC coatings via chemical vapour deposition (CVD) method. The ZrB_2 coating can be developed by employing a hydrogen reduction of $ZrCl_4$ and BCl_3 with argon gas as the carrier gas for the reactant vapour as per the following chemical reaction:

$$ZrCl_4 + 2BCl_3 + 5H_2 \rightarrow ZrB_2 + 10HCl$$

The precursors employed for the CVD method include $Zr(BH)_4$ and $Hf(BH)_4$, thus leading to the formation of ZrB_2 and HfB_2, respectively. By employing the CVD method, a group of researchers have developed TaC coatings on a C/C composite by maintaining a temperature beyond 2373 K. The study showed that the ablative characteristics of the UHTC coating thus prepared are highly altered by the morphology of crystal. The study also showed that an acicular crystal TaC coating exhibits excellent ablation resistance, while acute oxidation results in the conversion of the coating to its powder form [52]. The schematic representation of the CVD employed for the preparation of the UHTCs is shown in Fig. 5. With the selection of the precursors for the preparation of UHTCs, the reaction occurs within the reaction chamber at high temperature and results in the deposition of the UHTCs as depicted in Fig. 5.

5.2 Physical Vapour Deposition Method

In this method, the physical removal of a material from a sample by means of evaporation or ejection is used in preparing a thin film of UHTC coatings without incorporating chemical reactions. But it involves some procedures including high-temperature vacuum deposition, plasma sputtering, etc., to coat the UHTC material on the surface of a substrate. A sputtering method that involves the ejection of atoms from a solid material via collision with particle of high energy, was employed by researchers to form a UHTC thin film of ZrB_2 having a thickness of 800 nm on silicon substrate [54]. The schematic representation of the physical vapour deposition method for the preparation of UHTCs is shown in Fig. 6.

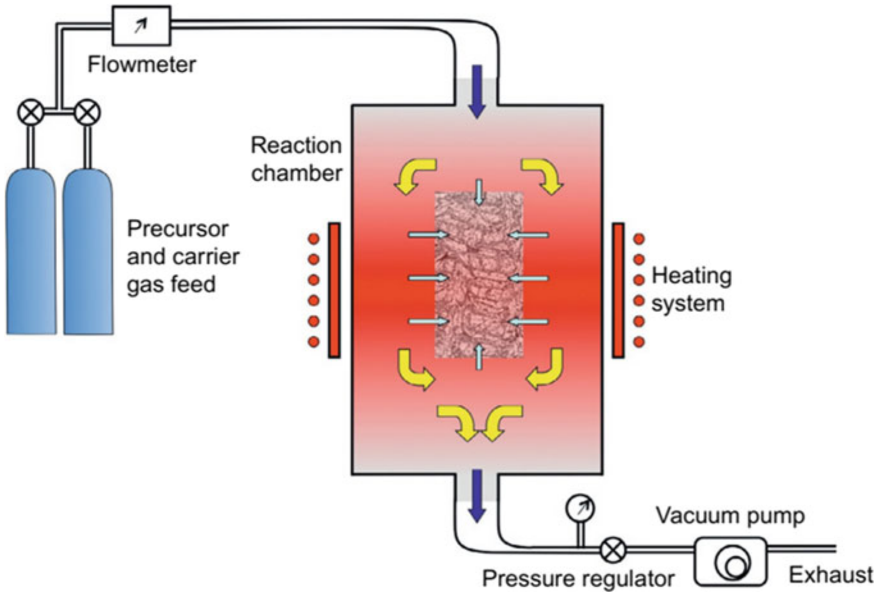

Fig. 5 Schematic representation of chemical vapour deposition/infiltration employed for the preparation of UHTCs [53]. Copyright 2015. Reproduced with permission from Elsevier

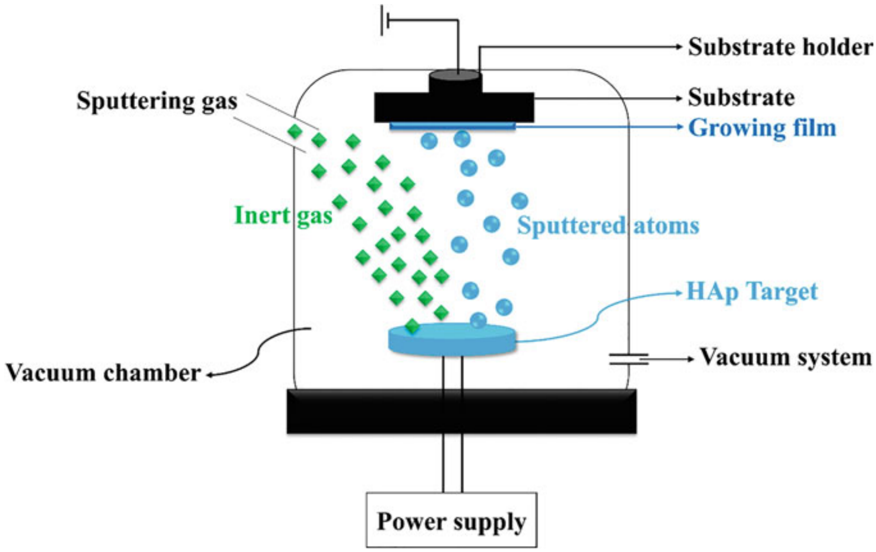

Fig. 6 Schematic of physical vapour deposition method for the preparation of UHTCs [55]. Copyright 2021. Reproduced with permission from MDPI

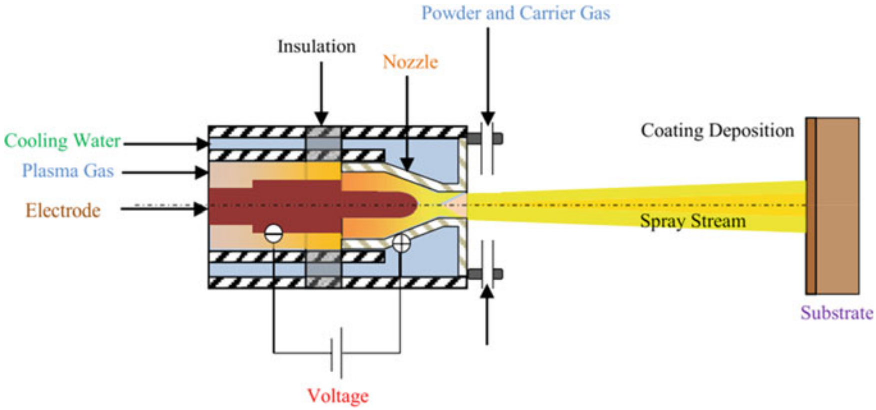

Fig. 7 Schematic of plasma gun employed for the preparation of UHTCs [57]. Copyright 2019. Reproduced with permission from Elsevier

5.3 Plasma Spray Method

This technique is employed in preparing UHTC coatings having large thickness, usually in the range of 4–5 mm. Through this method, it is also possible to develop free standing UHTC coatings by removing the substrate. The quality of developed coating depends mainly on the properties of starting powders employed for the development of UHTCs in powder form. The oxidation resistance of UHTC is improved by depositing them via vacuum plasma spray method. The schematic of plasma gun employed for the preparation of UHTCs is shown in Fig. 7. In one such study, a group of researchers have deposited a UHTC coating of HfC and TiC on a substrate via plasma spray technique. The materials exhibited excellent hardness and mechanical properties. The hardness of HfC and TiC coatings was 1650.70 HV and 753.60 HV, respectively, while for HfC and TiC layers in the multilayer sample, the values were 1563.50 HV and 1059.20 HV, respectively. The roughness values were estimated as 5.710 μm for HfC coating, 4.300 μm for TiC coating and 3.320 μm for HfC/TiC coatings [56]. The Vicker's hardness obtained for single and multilayer coatings of HfC, TiC and HfC/TiC is depicted in Fig. 8.

6 Properties of UHTCs

The popular UHTC materials such as borides, carbides and nitrides of transition metals possess diverse mechanical and thermodynamic properties, which need to be optimized for specific applications. The important mechanical and thermodynamic properties of UHTCs are described in the subsequent subsections.

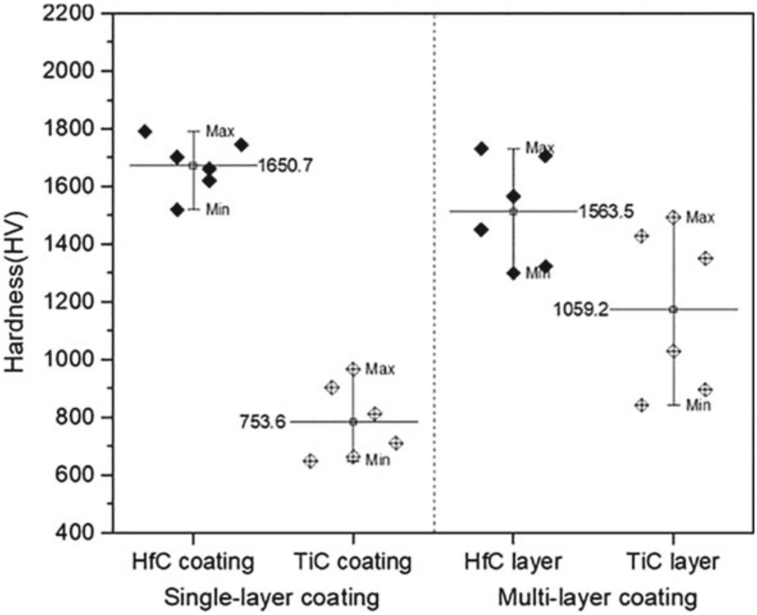

Fig. 8 Vicker's hardness of single and multilayer coatings of HfC, TiC and HfC/TiC formed by plasma spray method [56]. Copyright 2020. Reproduced with permission from MDPI

6.1 Mechanical Properties of UHTCs

Mechanical properties of UHTCs are of prime importance in various high-temperature applications. The important mechanical properties of UHTCs include elastic modulus, hardness, flexural strength, fracture toughness and grain size after sintering. The two mechanical properties of boride-based UHTCs, namely the elasticity and hardness are deeply related to the density of the material. However, the room temperature flexural strength depends on grain size of particles in UHTCs. But, grain size of particles is dependent on particle size at the initial stage, reinforcement phase content and the type of processing technique employed.

In a study, different composites composed of ZrB_2–B_4C were fabricated with 5, 15, 20 and 25 wt% of B_4C which were synthesised via a spark plasma sintering method at a temperature of 2273 K. All composite materials of ZrB_2–B_4C thus formed were fund to possess a relative density value in the range of 96.14–97.78%. However, adding B_4C to ZrB_2 matrix resulted in the improvement of the hardness of the composite material. The hardness of the composite material varied to a high value of 20 GPa when the wt% of B_4C is increased from 5 to 20. The fracture toughness of the composite material also varied from 2.93 MPa-m^0 to 4.13 MPa-m$^{0.5}$ when the wt% of B_4C is increased from 5 to 25. A highest machining speed of 10.56 mm^2/min was exhibited by the ZrB_2–25 wt% B_4C composite [58]. Nanoindentation can be employed to identify the mechanical properties of UHTCs. In a recent study, researchers have performed a nanoindentation under 6 strain rates to estimate the mechanical properties of UHTCs formed of the composite ZrB_2–SiC. The ZrB_2–SiC composite ceramic was fabricated by means of spark plasma sintering process and attained a relative density of 99.1%. The study showed that the hardness of the material increases with an increase in strain rate [59].

The joining of UHTC parts is a crucial process and it requires demanding conditions as it is difficult to manufacture large and complex components of the material. In a recent study, a Ni foil was employed as a filler to join UHTC parts and resulted in the fabrication of ZrB_2–SiC/Ni/ZrB_2–SiC (ZS/Ni/ZS) joint. The joint exhibited satisfactory mechanical properties by delivering a high shear strength, while the elastic modulus at the joint was found to be lower than that exhibited by the composite material. The oxidation resistance of the joint ZS/Ni/ZS joint was found to be extremely good, thus indicating that the joint can be employed for various experimental conditions over a range of temperature varying from 1073 to 1473 K [60]. In a recent research work, a sol–gel method was used in preparing UHTCs and developed a porous UHTC with grain size varying from 1 to 500 urn and a porosity in a range of 60% to 95% at a low temperature. This implies that the mechanical properties, specifically the grain properties, can be modified to a great extent by choosing a suitable synthesis method for UHTCs [41].

6.2 Thermal Shock Resistance of UHTCs

The brittleness of UHTCs leads to thermal shock failure of them under extreme conditions of temperature and pressure and is a critical concern when employed for various applications. Thermal shock fracture parameters and thermal shock damage parameters that define the thermal properties of UHTC materials. It is possible to improve the thermal shock resistance of the UHTCs by increasing its flexural strength keeping the elastic modulus, thermal expansion coefficient and the Poisson's ratio constant.

The thermal shock resistance of UHTCs can be improved by means of optimising the microstructure designs of the UHTC materials. The symmetric distribution of strong covalent bonds in UHTCs results in low damage resistance of UHTCs due to their intrinsic brittleness. Particle toughening is a suitable mechanism for improving the mechanical properties of UHTCs. In this method, the addition of second phase dispersion particles improves the corrosion and impact resistance of UHTCs. The toughening of whiskers is another mechanism by means of which the hardness, elastic modulus, tensile strength and thermal shock resistance of the UHTCs can be improved largely. A study employed slurry injection in combination with vacuum infiltration for developing carbon filler-reinforced ZrB_2–SiC ceramics. An improvement in mechanical properties of the composite ceramics ZrB_2–SiC was achieved via a homogeneous distribution between the nanofiller and the ceramics. A critical thermal shock temperature difference of 1087 K was attained, which is found to be greater than that for the traditional ZrB_2 based ceramics [61]. In another recent research work, the researchers have improved the thermal shock resistance of a ZrB_2–SiC–Al_3BC_3 UHTC synthesised via spark plasma sintering. The critical shock resistance temperature of the sample was found to be increasing with an increase in sintering temperature. In addition, the other mechanical properties of the material such as fracture toughness and flexural strength were also found to be improved to a great extent. The critical thermal shock resistance temperature of the specimen was found to be 865 K [62].

7 Simulation and Modelling Studies on UHTCs

The temperature distribution during the sintering process for the densification of UHTCs is very crucial as it decides the application suitability of many UHTCs. A prior numerical analysis will enable the researchers to identify the corns and pros of employing a particular technique for synthesis, densification or coating of UHTCs. The microstructure and the other related thermodynamic properties of the prepared sample are determined largely by the distribution temperature within the sample. Hence, in a study, researchers have performed a numerical analysis of the temperature distribution TiB_2 UHTCs during the densification process by employing a spark plasma sintering method. In this study, the current density distribution and the generated heat arising from Joule heating effect were determined during spark plasma sintering process. By employing a finite element method, it was identified that the point where the specimen is camped to the die produces high heat and it dissipates to the sample from the centre and finally to the surroundings. A homogeneous temperature distribution was identified in the sample and the maximum temperature difference was 348 K at the sample/die interface when maintaining a sintering temperature of 2473 K [63]. A numerical study was conducted on SPS of a cylindrical sample of TiC. A finite element method was employed for solving differential equations such as heat diffusion equation and the electricity distribution equation. Stefan Boltzmann law and Newton's cooling law were employed to solve the radiation heat transfer and the convective cooling mechanisms. The study showed that the temperature of the sample is maximum at the centre. A gradient distribution of temperature was identified in the sample along the radial direction with the minimum and the maximum values of temperature as 2193 K and 2273 K, respectively, while no gradient distribution of temperature was noticed along the vertical direction [64].

The effect of flaws on the flexural strength of UHTCs can be modelled via a numerical modelling and analysis. In a numerical modelling study, the UHTC composite materials, ZrB_2, ZrB_2–SiC and ZrB_2–SiC–G composed of micro flaws, with adjustable size, shape and orientation have been modelled considering the properties of the material and the geometry of the flaws. The study indicated that the flaws have an impact on the flexural strength of the UHTC can be estimated from the value of elastic modulus and the related mechanical properties [65]. A phase field numerical modelling study was employed to measure the fracture toughness of the ZrB_2–C ceramics possessing various engineered microarchitectures. The modelling study was verified by considering a fibrous monolith consisting of various volume fractions of C-rich phase. The modelled samples containing 10 and 30 vol% of C-rich phase exhibited an effective fracture toughness values 42% above than that of pure ZrB_2 sample. If the C-rich phase is increased further to 50 vol%, the fracture toughness value was found to drop to a great extent as per the numerical study and was validated from the experimental results also [66].

A recent modelling study based on the finite element method with the governing equations such as balanced heat equation and transport equation was employed to analyse the suitability of UHTCs in hypersonic flight conditions. The mathematical modelling study was performed on the assumptions that the induced porosity follows the linear and parabolic solutions of Laplace equations. The critical heat flux for the modelling study was varied between 7 and 44 MW/m^2. Simulation study was performed for four diverse UHTC composites and the results indicated a temperature rise crossing 4973 K along with a deformation on the fixed area where the heat flux was developed. A reduction in deformation was noticed with a variation in porosity of the UHTC material. The study also identified that porous UHTCs possess excellent thermal shock resistance owing to the release of thermal shock via the existing pores in the material [67]. Temperature sensitive interior components can be developed for hypersonic flight applications. Dense UHTCs can be employed for thermal protection at the leading edges of hypersonic flights, while porous UHTCs can be employed for developing thermally insulated interfaces for their interior components. Designing suitable hypersonic vehicles require the modification of their thermodynamic properties over a range of temperature from 253 to 2773 K. A material point method can be employed for numerical modelling for analysing the temperature dependence of properties of materials with consisting of damage and in the absence of damage. The model involves the significance of micro buckling for estimating the stiffness and thermal conductivity of the UHTC material [68]. The ABAQUS software can be employed for simulating the ultra-high-temperature thermal field of loaded aircraft moving at ultra-high speed [69].

Machine learning (ML) algorithm has been employed for predicting Young's modulus, flexural strength and fracture toughness for various processing parameters, mixture selections as well as testing parameters. An accurately trained ML model can predict mechanical properties of UHTC materials properly. ML studies have shown that the prediction performance of the ML algorithms for the Young's modulus is superior when compared to that for flexural strength and fracture toughness [70]. A three-dimensional thermomechanical phase field model (PFM) was developed for analysing the thermal shock-induced fracture by considering the dependence of properties of material on temperature. This model is completely different from other PFMs due to the fact that it can remove the unexpected damage evolution by introducing a fracture energy threshold, which is completely dependent on temperature. Thus, the PFM study shows that the tensile part of the strain energy is dominant over the thermal shock-induced cracks in UHTCs [71].

8 Applications of UHTCs

In the aerospace applications, UHTCs play a prominent role in developing the thermal protection systems. It can be employed for various other applications including transpiration cooling and other high entropy applications. Some interesting recent applications of UHTCs are summarised in the following subsections.

8.1 Oxidation Protective UHTC Coatings

Carbon–carbon (C–C) composites are useful materials for hypersonic flight vehicles; however, they undergo oxidation in the presence of air at temperature above 773 K. They require excellent heat protection system to overcome aerothermal heating under high-temperature environment. The C–C composites can be thermally protected from oxidation by employing a UHTC coating material formed of ZrB_2 and SiC. In a method employed in this direction, researchers have combined pre-treatment and processing steps to develop continuous and adherent high-temperature coatings from infiltrated preceramic polymers. The protective coatings were tested at 2873 K and were identified as extremely beneficial for resistance against oxidation in such high-temperature applications [72]. In another study, the ablation-oxidation resistance of carbon fibre (Cf)/C matrix (C)–SiC–TiC–TaC ceramic matrix composite was developed by melt infiltration of alloy into a Cf/C preform and tested for various oxidation conditions. The test conditions include an oxyacetylene flame shot of 7.5 s duration fulfilled by a radiant furnace in air at 1873 K up to 480 s. The study showed an improvement in ablation-oxidation resistance of one order of magnitude for the oxidised/ablated ceramic matrix composite when compared to the unprotected one. The CMC can be employed for various aerospace and hypersonic applications [73].

A three-layer SiC/UHTC/SiC coating was prepared for the protection of C/SiC composites for a long duration over a temperature range of 1373 K to 1773 K. A novel sintering technique was employed to densify a ZrB_2 UHTC in presence of a gaseous mixture of 70 vol% Ar and 30 vol% air. A mass loss of 0.36, 1.65 and 3.45 mg cm^{-2} was reported when the composite UHTC material is exposed to air for 114 h at 1373 K, 114 h at 1573 K and 68 h at 1773 K, respectively. The low mass loss rate arises from the beneficial properties of both ZrB_2 and SiC layers [72].

8.2 Thermal Barrier UHTC Coatings

Thermal insulation under extreme conditions is useful for carbon aerogel and are characterised by brittleness and ease of fabrication. A sol–gel polymerisation of phenolic resin and siloxane resulted in silica modified carbon aerogels (SCAs). This process is followed by pressure drying and carbonisation. The study involves an estimation of the density of the SCA and is found to possess a high density of 0.5 g/ cm^3 and a mean pore size of 33 nm. The oxidation resistance of carbon aerogels can be improved to a great extent via the transformation of siloxane to amorphous SiO_2 particles and crystalline SiC particles that can coated on the surface of carbon nanoparticles during the carbonisation process. SCAs possess a high thermal conductivity and excellent compressive strength. They can act as an excellent thermal barrier under extremely harsh environmental conditions [74]. In a study, a novel method was proposed to improve the thickness of thermal barrier coating locally in the hotspot areas for enhancing thermal insulation and life capabilities of combustor tiles. This method involves the inclusion of a pre dent for adding an extra thickness to the thermal barrier coating. The study showed a thickness dependent temperature reduction by 13% on the addition of pre dent, which in turn provided a performance improvement of 3% [75]. A few studies have reported the development of thermal barrier UHTCs using various methods [76, 77].

9 High Entropy UHTCs

The concept of high entropy UHTCs was derived from the existence of high entropy alloys. In a high entropy alloy, there exists five or more elements in equimolar or non-equimolar concentration, which in turn make the material to possess high configurational entropy. This also help them to form single phase solid solution with some basic crystal structures such as FCC, BCC etc. There exists a wide range of high entropy ceramic materials such as high entropy borides, carbides, silicides, fluorides, diborides etc. The high entropy diborides and carbides such as ZrB_2, HfB_2, ZrC, HfC and TaC represent high entropy UHTCs. The first high entropy boride was reported in 2016 and fabricated in 2018 [78, 79]. The synthesised high entropy diborides exhibit a hexagonal crystal structure and the high entropy carbides exhibit a FCC structure.

9.1 Properties of High Entropy UHTCs

The mechanical properties of high entropy UHTCs are largely dependent on the microstructure of the ceramics. The Vicker's hardness of high entropy UHTCs with high density of found to be 20–35 GPa. High entropy UHTCs can be employed for thermal barrier coating applications owing to their excellent thermal shock resistance and oxidation resistance properties. The fibre-reinforced high entropy UHTCs possess excellent mechanical properties and can be employed for various high-temperature applications. This also removes the intrinsic brittleness of bulk UHTCs. Some studies have shown that the thermal conductivity of high entropy UHTCs is lower than that of the individual metal diborides and carbides. The presence of oxygen content can also affect the thermal conductivity of high entropy UHTCs. A

Table 1 Comparison of properties of high entropy UHTCs [82]

Material	M_{exp} [GPa]	H_{exp} [GPa]
HfC	552 ± 15	31.5 ± 1.3
TaC	579 ± 20	20.6 ± 1.2
ZrC	507 ± 16	31.3 ± 1.4
NbC	585 ± 23	27.2 ± 1.7
(Hf–Ta)C	559 ± 18	32.9 ± 1.8
(Hf–Ta–Zr–Nb)C	598 ± 15	36.1 ± 1.6
Rule of mixture (HfC, TaC, ZrC, NbC)	556	27.7

study has shown that the addition graphite can eliminate the oxygen impurity and improve the thermal conductivity of high entropy UHTCs [80].

The oxidation resistance of high entropy UHTC materials is found to be better than that of the individual diborides and carbides [78]. Due to the presence of a several elements in the high entropy ceramics, they exhibit compositional diversity, which in turn can help to improve the oxidation resistance of these materials. The addition of SiC to the high entropy UHTCs improves the oxidation resistance via the formation of an oxide layer coating for the UHTC material [81]. A comparison of experimental values of the properties such as indentation modulus (M) and hardness (H) of various high-temperature UHTCs is listed in Table 1.

9.2 Applications of High Entropy UHTCs and Future Research Directions

High entropy UHTCs can also exist in diverse forms such as ceramic form, coatings, thin films, fibre-reinforced composite coating form etc. The fibre-reinforced high entropy UHTC coatings possess excellent mechanical properties owing to the oxidation resistance of the high entropy UHTC material. The future research studies must focus on the high entropy UHTCs and the fibre-reinforced high entropy UHTC coatings because of their unique mechanical and thermodynamic properties. Not much studies have been done so far on the high entropy UHTCs and high entropy UHTC coatings. The studies done so far on these materials are very scarce, which in turn hinders the application of these materials under high-temperature environments.

10 Summary and Outlooks

This chapter focuses on the recent advances in UHTCs in various applications under very high-temperature environments. The borides, nitrides and carbides of various transition metals can be employed for synthesising ultra-high-temperature ceramic (UHTC) coatings and a brief overview of these materials is included in this chapter. These materials possess excessively high melting point along with excellent mechanical properties at extremely high temperature, including excellent intrinsic brittleness and hardness. The extremely poor shock resistance of bulk ceramics can be overcome to a greater extent with the application of ultra-high-temperature ceramic coatings and fibre-reinforced ultra-high-temperature ceramics. UHTC coatings are extremely useful as thermal shock absorbers, surface seals and leak minimisers. The chapter also summarises the different synthesis methods, densification methods and coating methods that can be employed for UHTCs. The solid-state powders-based and solution-based methods have been employed recently to enhance the unique properties of them. The synthesis methods face a few challenges and require highly refined approaches to synthesis high purity UHTC powders, suitable chemical synthesis reactions and proper selection of precursors delivering excellent chemical yield and less degradation. Apart from the excellent mechanical properties such as excellent elasticity, flexural strength and fracture toughness, the UHTCs must be assessed for its machinability when they are employed for hypersonic and space applications. Oxidation resistance at high-temperature environment is the most wanted property of materials especially when they are employed for various space applications. This chapter also summarised the mechanical and thermodynamic properties of UHTCs.

Recent advances show that the use of multilayers of the high-temperature ceramic protective coating reduces the oxidation of carbon–carbon (C–C) composites and protect them from aerothermal heating at temperatures above 3273 K. Hence, the mechanisms, kinetics and the end products of oxidation mechanisms help the researchers to identify the strengths and weaknesses of the UHTCs when employed for specific applications. A brief overview of the computational studies done so far on UHTCs for estimating and validating their mechanical and thermodynamical properties is also mentioned in this chapter. The atomistic computational modelling and simulation studies on the impacts of defects on the thermal and mechanical properties of UHTCs are found to be extremely useful to identify their drawbacks prior to their employment in various device configurations. In a similar way, the computational studies on UHTCs by employing thermal shock modelling tools provide useful information about their thermal shock resistance. This chapter also provides a brief overview of the applications of UHTCs along with a description of the properties and applications of the emerging high entropy UHTCs.

References

1. Belmonte, M.: Advanced ceramic materials for high temperature applications. Adv. Eng. Mater. **8**, 693–770 (2006). https://doi.org/10.1002/adem.200500269
2. Eakins, E., Jayaseelan, D.D., Lee, W.E.: Toward oxidation-resistant ZrB_2–SiC ultra high temperature ceramics. Metall. Mater. Trans. A. **42**, 878–887 (2011). https://doi.org/10.1007/s11661-010-0540-8
3. Guo, S.Q.: Densification of ZrB_2-based composites and their mechanical and physical properties: a review. J. Eur. Ceram. **29**, 995–1011 (2009). https://doi.org/10.1016/j.jeurceramsoc.2008.11.008
4. Thimmappa, S.K., Golla, B.R.: Oxidation behavior of silicon-based ceramics reinforced diboride UHTC: a review. Silicon 1–26 (2022). https://doi.org/10.1007/s12633-022-01945-8
5. Ni, D., Cheng, Y., Zhang, J., Liu, J.X., Zou, J., Chen, B., Wu, H., Li, H., Dong, S., Han, J., Zhang, X.: Advances in ultra-high temperature ceramics, composites, and coatings. J. Adv. Ceram. **11**, 1–56 (2022). https://doi.org/10.1007/s40145-021-0550-6
6. Fahrenholtz, W.G., Hilmas, G.E.: Ultra-high temperature ceramics: materials for extreme environments. Scr. Mater. **129**, 94–99 (2017). https://doi.org/10.1016/j.scriptamat.2016.10.018
7. Zhang, X., Hu, P., Han, J., Meng, S.: Ablation behavior of ZrB_2–SiC ultra high temperature ceramics under simulated atmospheric re-entry conditions. Compos. Sci. Technol. **68**, 1718–1726 (2008). https://doi.org/10.1016/j.compscitech.2008.02.009
8. Opeka, M.M., Talmy, I.G., Wuchina, E.J., Zaykoski, J.A., Causey, S.J.: Mechanical, thermal, and oxidation properties of refractory hafnium and zirconium compounds. J. Eur. Ceram. **19**, 2405–2414 (1999). https://doi.org/10.1016/S0955-2219(99)00129-6
9. Van Wie, D.M., Drewry, D.G., King, D.E., Hudson, C.M.: The hypersonic environment: required operating conditions and design challenges. J. Mater. Sci. **39**, 5915–5924 (2004). https://doi.org/10.1023/B:JMSC.0000041688.68135.8b
10. Wuchina, E., Opila, E., Opeka, M., Fahrenholtz, B., Talmy, I.: UHTCs: ultra-high temperature ceramic materials for extreme environment applications. The Electrochem. Soc. Interface. **16**, 30 (2007). https://doi.org/10.1149/2.F04074IF
11. Mao, H., Shen, F., Zhang, Y., Wang, J., Cui, K., Wang, H., Lv, T., Fu, T., Tan, T.: Microstructure and mechanical properties of carbide reinforced TiC-based ultra-high temperature ceramics: a review. Coatings **11**, 1444 (2021). https://doi.org/10.3390/coatings11121444
12. Tului, M., Lionetti, S., Pulci, G., Rocca, E., Valente, T., Marino, G.: Effects of heat treatments on oxidation resistance and mechanical properties of ultra-high temperature ceramic coatings. Surf. Coat. Technol. **202**, 4394–4398 (2008). https://doi.org/10.1016/j.surfcoat.2008.04.015
13. Tului, M., Lionetti, S., Pulci, G., Marra, F., Tirillò, J., Valente, T.: Zirconium diboride based coatings for thermal protection of re-entry vehicles: effect of $MoSi_2$ addition. Surf. Coat. Technol. **205**, 1065–1069 (2010). https://doi.org/10.1016/j.surfcoat.2010.07.120
14. Chamberlain, A.L., Fahrenholtz, W.G., Hilmas, G.E., Ellerby, D.T.: High-strength zirconium diboride-based ceramics. J. Am. Ceram. **87**, 1170–1172 (2004). https://doi.org/10.1111/j.1551-2916.2004.01170.x
15. Carney, C., Paul, A., Venugopal, S., Parthasarathy, T., Binner, J., Katz, A., Brown, P.: Qualitative analysis of hafnium diboride based ultra high temperature ceramics under oxyacetylene torch testing at temperatures above 2100 °C. J. Eur. Ceram. **34**, 1045–1051 (2014). https://doi.org/10.1016/j.jeurceramsoc.2013.11.018
16. Balbo, A., Sciti, D.: Spark plasma sintering and hot pressing of ZrB_2–$MoSi_2$ ultra-high-temperature ceramics. Mater. Sci. Eng.: A **475**, 108–112 (2008). https://doi.org/10.1016/j.msea.2007.01.164
17. Sciti, D., Guicciardi, S., Nygren, M.: Densification and mechanical behavior of HfC and HfB_2 fabricated by spark plasma sintering. J. Am. Ceram. **91**, 1433–1440 (2008). https://doi.org/10.1111/j.1551-2916.2007.02248.x
18. Shen, L., Zhao, Y., Li, Y., Wu, H., Zhu, H., Xie, Z.: Synergistic strengthening of FeCrNiCo high entropy alloys via micro-TiC and nano-SiC particles. Mater. Tod. Commun. **26**, 101729 (2021). https://doi.org/10.1016/j.mtcomm.2020.101729

19. Gholizadeh, T., Vajdi, M., Rostamzadeh, H.: A new trigeneration system for power, cooling, and freshwater production driven by a flash-binary geothermal heat source. Renew. Energ. **148**, 31–43 (2020). https://doi.org/10.1016/j.renene.2019.11.154
20. Cui, K., Zhang, Y., Fu, T., Wang, J., Zhang, X.: Toughening mechanism of mullite matrix composites: a review. Coatings **10**, 672 (2020). https://doi.org/10.3390/coatings10070672
21. Cui, K., Mao, H., Zhang, Y., Wang, J., Wang, H., Tan, T., Fu, T.: Microstructure, mechanical properties, and reinforcement mechanism of carbide toughened ZrC-based ultra-high temperature ceramics: a review. Compos. Interfaces. **29**, 729–748 (2022). https://doi.org/10.1080/09276440.2021.2012409
22. Musa, C., Licheri, R., Orrù, R., Cao, G., Balbo, A., Zanotto, F., Mercatelli, L., Sani, E.: Optical characterization of hafnium boride and hafnium carbide-based ceramics for solar energy receivers. Sol. Energy. **169**, 111–119 (2018). https://doi.org/10.1016/j.solener.2018.04.036
23. Fahrenholtz, W.G.: Thermodynamic analysis of ZrB_2–SiC oxidation: formation of a SiC-depleted region. J. Am. Ceram. **90**, 143–148 (2007). https://doi.org/10.1111/j.1551-2916.2006.01329.x
24. Fahrenholtz, W.G.: The ZrB_2 volatility diagram. J. Am. Ceram. **88**, 3509–3512 (2005). https://doi.org/10.1111/j.1551-2916.2005.00599.x
25. Zeng, Y., Wang, D., Xiong, X., Zhang, X., Withers, P.J., Sun, W., Smith, M., Bai, M., Xiao, P.: Ablation-resistant carbide $Zr_{0.8}Ti_{0.2}C_{0.74}B_{0.26}$ for oxidizing environments up to 3000 °C. Nat. Commun. **8**, 15836 (2017). https://doi.org/10.1038/ncomms15836
26. Zhang, B., Yin, J., Zheng, J., Liu, X., Huang, Z., Dusza, J., Jiang, D.: High temperature ablation behavior of pressureless sintered $Ta_{0.8}Hf_{0.2}C$-based ultra-high temperature ceramics. J. Eur. Ceram. **40**, 1784–1789 (2020). https://doi.org/10.1016/j.jeurceramsoc.2019.11.043
27. Singh, A., Kuppusami, P., Khan, S., Sudha, C., Thirumurugesan, R., Ramaseshan, R., Divakar, R., Mohandas, E., Dash, S.: Influence of nitrogen flow rate on microstructural and nanomechanical properties of Zr–N thin films prepared by pulsed DC magnetron sputtering. Appl. Surf. Sci. **280**, 117–123 (2013). https://doi.org/10.1016/j.apsusc.2013.04.107
28. Yoshitake, M., Yotsuya, T.Y.T., Ogawa, S.O.S.: Effects of nitrogen pressure and RF power on the properties of reactive magnetron sputtered Zr–N films and an application to a thermistor. Jpn. J. Appl. Phys. **31**, 4002 (1992). https://doi.org/10.1143/JJAP.31.4002
29. Peters, A.B., Wang, C., Zhang, D., Hernandez, A., Nagle, D.C., Mueller, T., Spicer, J.B.: Reactive laser synthesis of ultra-high-temperature ceramics HfC, ZrC, TiC, HfN, ZrN, and TiN for additive manufacturing. Ceram. Int. **49**, 11204–11229 (2023). https://doi.org/10.1016/j.ceramint.2022.11.319
30. Buinevich, V.S., Nepapushev, A.A., Moskovskikh, D.O., Trusov, G.V., Kuskov, K.V., Vadchenko, S.G., Rogachev, A.S., Mukasyan, A.S.: Fabrication of ultra-high-temperature nonstoichiometric hafnium carbonitride via combustion synthesis and spark plasma sintering. Ceram. Int. **46**, 16068–16073 (2020). https://doi.org/10.1016/j.ceramint.2020.03.158
31. Sonber, J.K., Murthy, T.C., Subramanian, C., Hubli, R.C., Suri, A.K.: Processing methods for ultra-high temperature ceramics. In: MAX phases and ultra-high temperature ceramics for extreme environments (180–202). IGI Global (2013). https://doi.org/10.4018/978-1-4666-4066-5.ch006
32. Brochu, M., Gauntt, B., Zimmerly, T., Ayala, A., Loehman, R.: Fabrication of UHTCs by conversion of dynamically consolidated Zr+ B and Hf+ B powder mixtures. J. Am. Ceram. **91**, 2815–2822 (2008). https://doi.org/10.1111/j.1551-2916.2008.02550.x
33. Anselmi-Tamburini, U., Kodera, Y., Gasch, M., Unuvar, C., Munir, Z.A., Ohyanagi, M., Johnson, S.M.: Synthesis and characterization of dense ultra-high temperature thermal protection materials produced by field activation through spark plasma sintering (SPS): I. Hafnium diboride I. J. Mater. Sci. **41**, 3097–3104 (2006). https://doi.org/10.1007/s10853-005-2457-y
34. Millet, P., Hwang, T.: Preparation of TiB_2 and ZrB_2. Influence of a mechano-chemical treatment on the borothermic reduction of titania and zirconia. J. Mater. Sci. **31**, 351–355 (1996). https://doi.org/10.1007/BF01139151
35. Khanra, A.K., Pathak, L.C., Godkhindi, M.M.: Carbothermal synthesis of zirconium diboride (ZrB_2) whiskers. Adv. Appl. Ceram. **106**, 155–160 (2007). https://doi.org/10.1179/174367607X162019

36. Guo, W.M., Zhang, G.J.: Reaction processes and characterization of ZrB_2 powder prepared by boro/carbothermal reduction of ZrO_2 in vacuum. J. Am. Ceram. **92**, 264–267 (2009). https://doi.org/10.1111/j.1551-2916.2008.02836.x
37. Khanra, A.K., Pathak, L.C., Mishra, S.K., Godkhindi, M.M.: Sintering of ultrafine zirconium diboride powder prepared by modified SHS technique. Adv. Appl. Ceram. **104**, 282–284 (2005). https://doi.org/10.1179/174367605X52077
38. Xie, Y., Sanders, T.H., Jr., Speyer, R.F.: Solution-based synthesis of submicrometer ZrB_2 and ZrB_2–TaB_2. J. Am. Ceram. **91**, 1469–1474 (2008). https://doi.org/10.1111/j.1551-2916.2008.02288.x
39. Devyatkin, S.V.: Electrosynthesis of zirconium boride from cryolite–alumina melts containing zirconium and boron oxides. Russ. J. Electrochem. **37**, 1308–1311 (2001). https://doi.org/10.1023/A:1013295931573
40. Su, K., Sneddon, L.G.: Polymer-precursor routes to metal borides: synthesis of titanium boride (TiB_2) and zirconium boride (ZrB_2). Chem. Mater. **3**, 10–12 (1991). https://doi.org/10.1021/cm00013a005
41. Li, F., Huang, X., Liu, J.X., Zhang, G.J.: Sol–gel derived porous ultra-high temperature ceramics. J. Adv. Ceram. **9**, 1–16 (2020). https://doi.org/10.1007/s40145-019-0332-6
42. Mashhadi, M., Khaksari, H., Safi, S.: Pressureless sintering behavior and mechanical properties of ZrB_2–SiC composites: effect of SiC content and particle size. J. Mater. Res. **4**, 416–422 (2015). https://doi.org/10.1016/j.jmrt.2015.02.004
43. Mazur, P., Grigoriev, O., Vedel, D., Melakh, L., Shepa, I.: Ultra-high temperature ceramics based on ZrB_2 obtained by pressureless sintering with addition of Cr_3C_2, Mo_2C, and WC. J. Eur. Ceram. **42**, 4479–4492 (2022). https://doi.org/10.1016/j.jeurceramsoc.2022.04.043
44. Peters, A.B., Wang, C., Zhang, D., Hernandez, A., Nagle, D.C., Mueller, T., Spicer, J.B.: Reactive laser synthesis of ultra-high-temperature ceramics HfC, ZrC, TiC, HfN, ZrN, and TiN for additive manufacturing. Ceram. Int. **49**, 11204–11229 (2022). https://doi.org/10.1016/j.ceramint.2022.11.319
45. Hu, P., Gui, K., Hong, W., Zhang, X., Dong, S.: High-performance ZrB_2–SiC–Cf composite prepared by low-temperature hot pressing using nanosized ZrB_2 powder. J. Eur. Ceram. **37**, 2317–2324 (2017). https://doi.org/10.1016/j.jeurceramsoc.2017.02.008
46. Lee, S.J., Kang, E.S., Baek, S.S., Kim, D.K.: Reactive hot pressing and oxidation behavior of Hf-based ultra-high-temperature ceramics. Surf. Rev. Let. **17**, 215–221 (2010). https://doi.org/10.1142/S0218625X10013886
47. Guillon, O., Gonzalez-Julian, J., Dargatz, B., Kessel, T., Schierning, G., Räthel, J., Herrmann, M.: Field-assisted sintering technology/spark plasma sintering: mechanisms, materials, and technology developments. Adv. Eng. Mater. **16**, 830–849 (2014). https://doi.org/10.1002/adem.201300409
48. Zhao, X., Zou, J., Ji, W., Wang, A., He, Q., Xiong, Z., Wang, W., Fu, Z.: Processing and mechanical properties of B_4C–SiCw ceramics densified by spark plasma sintering. J. Eur. Ceram. **42**, 2004–2014 (2022). https://doi.org/10.1016/j.jeurceramsoc.2022.01.003
49. Vasudevan, N., Ahamed, N.N.N., Pavithra, B., Aravindhan, A., Shanmugavel, B.P.: Effect of Ni addition on the densification of TiC: a comparative study of conventional and microwave sintering. IJRMHM. **87**, 105165 (2020). https://doi.org/10.1016/j.ijrmhm.2019.105165
50. Sharma, A., Karunakar, D.B.: Development and characterizations of ZrB_2–SiC composites sintered through microwave sintering. In: Advances in manufacturing and industrial engineering: select proceedings of ICAPIE 2019 (pp. 815–824). Springer Singapore (2021). https://doi.org/10.1007/978-981-15-8542-5_71
51. Sun, C.N., Baldridge, T., Gupta, M.C.: Fabrication of ZrB_2–Zr cermet using laser sintering technique. Mater. Let. **63**, 2529–2531 (2009). https://doi.org/10.1016/j.matlet.2009.08.059
52. Zhang, Y., Gai, W., Wang, H., Chen, G., Zhang, P., Li, H.: Influence of crystallite morphology on the ablative behaviors of CVD-TaC coatings prepared on C/C composites beyond 2100 °C. Corros. Sci. **205**, 110426 (2022). https://doi.org/10.1016/j.corsci.2022.110426
53. Vignoles, G.L.: Chemical vapor deposition/infiltration processes for ceramic composites. In: Advances in Composites Manufacturing and Process Design, pp. 147–176. Woodhead Publishing (2015). https://doi.org/10.1016/B978-1-78242-307-2.00008-7

54. Shappirio, J.R., Finnegan, J.J.: Synthesis and properties of some refractory transition metal diboride thin films. Thin Solid Films **107**, 81–87 (1983). https://doi.org/10.1016/0040-6090(83)90010-X
55. Safavi, M.S., Walsh, F.C., Surmeneva, M.A., Surmenev, R.A., Khalil-Allafi, J.: Electrodeposited hydroxyapatite-based biocoatings: recent progress and future challenges. Coatings **11**, 110 (2021). https://doi.org/10.3390/coatings11010110
56. Kim, H.S., Kang, B.R., Choi, S.M.: Microstructure and mechanical properties of vacuum plasma sprayed HfC, TiC, and HfC/TiC ultra-high-temperature ceramic coatings. Materials **13**, 124 (2019). https://doi.org/10.3390/ma13010124
57. Ranjan, A., Islam, A., Pathak, M., Khan, M.K., Keshri, A.K.: Plasma sprayed copper coatings for improved surface and mechanical properties. Vacuum **168**, 108834 (2019). https://doi.org/10.1016/j.vacuum.2019.108834
58. Mandal, S., Chakraborty, S., Dey, P.: A study of mechanical properties and WEDM machinability of spark plasma sintered ZrB_2–B_4C ceramic composites. Micron **153**, 103198 (2022). https://doi.org/10.1016/j.micron.2021.103198
59. Jin, X., Wang, X., Liu, L., Yin, Y., Wang, H., Zhang, B., Fan, X.: Strain rate effect on the mechanical properties of ZrB_2–SiC ceramics characterized by nanoindentation. Ceram. Int. **48**, 10333–10338 (2022). https://doi.org/10.1016/j.ceramint.2022.01.331
60. Jin, X., Yang, J., Sun, Y., Li, P., Hou, C., Zhao, Y., Fan, X.: Fabrication and characterisation of high-performance joints made of ZrB_2–SiC ultra-high temperature ceramics. J. Eur. Ceram. **41**, 7412–7422 (2021). https://doi.org/10.1016/j.jeurceramsoc.2021.08.018
61. Zhang, D., Feng, J., Hu, P., Xun, L., Liu, M., Dong, S., Zhang, X.: Enhanced mechanical properties and thermal shock resistance of Cf/ZrB_2–SiC composite via an efficient slurry injection combined with vibration-assisted vacuum infiltration. J. Eur. Ceram. **40**, 5059–5066 (2020). https://doi.org/10.1016/j.jeurceramsoc.2020.07.003
62. Zhao, X., Chen, Z., Wang, H., Zhang, Z., Shao, G., Zhang, R., Fan, B., Lu, H., Xu, H., Chen, D.: The influence of additive and temperature on thermal shock resistance of ZrB_2 based composites fabricated by spark plasma sintering. Mater. Chem. Phys. **240**, 122061 (2020). https://doi.org/10.1016/j.matchemphys.2019.122061
63. Fattahi, M., Ershadi, M.N., Vajdi, M., Moghanlou, F.S., Namini, A.S., Asl, M.S.: On the simulation of spark plasma sintered TiB_2 ultra high temperature ceramics: a numerical approach. Ceram. Int. **46**, 14787–14795 (2020). https://doi.org/10.1016/j.ceramint.2020.03.003
64. Bagheri, S.M., Vajdi, M., Moghanlou, F.S., Sakkaki, M., Mohammadi, M., Shokouhimehr, M., Asl, M.S.: Numerical modeling of heat transfer during spark plasma sintering of titanium carbide. Ceram. Int. **46**, 7615–7624 (2020). https://doi.org/10.1016/j.ceramint.2019.11.262
65. Wang, A., Zhao, X., Huang, M., Zhang, Z., Xie, L.: A quantitative study of flaw/strength response in ultra-high temperature ceramics based on femtosecond laser method. Theor. Appl. Fract. Mech. **110**, 102775 (2020). https://doi.org/10.1016/j.tafmec.2020.102775
66. Emdadi, A., Watts, J., Fahrenholtz, W.G., Hilmas, G.E., Zaeem, M.A.: Predicting effective fracture toughness of ZrB_2-based ultra-high temperature ceramics by phase-field modeling. Mater. Des. **192**, 108713 (2020). https://doi.org/10.1016/j.matdes.2020.108713
67. Zuccarini, C., Ramachandran, K., Russo, S., Jayakody, Y.C., Jayaseelan, D.D.: Mathematical modeling and simulation of porosity on thermomechanical properties of UHTCs under hypersonic conditions. IJCES. **5**, e10168 (2023). https://doi.org/10.1002/ces2.10168
68. Povolny, S.J., Seidel, G.D., Tallon, C.: Numerical investigation of thermomechanical response of multiscale porous ultra-high temperature ceramics. Ceram. Int. **48**, 11502–11517 (2022). https://doi.org/10.1016/j.ceramint.2022.01.006
69. Liu, B., Wang, Y., Li, C., Tian, Z., Cheng, L.: Research on the thermal shock simulation of the super high-speed aircraft. MAMS. 1–8 (2022). https://doi.org/10.1080/15376494.2022.2046218
70. Han, T., Huang, J., Sant, G., Neithalath, N., Kumar, A.: Predicting mechanical properties of ultrahigh temperature ceramics using machine learning. J. Am. Ceram. **105**, 6851–6863 (2022). https://doi.org/10.1111/jace.18636

71. Li, D., Li, P., Li, W., Li, W., Zhou, K.: Three-dimensional phase-field modeling of temperature-dependent thermal shock-induced fracture in ceramic materials. Eng. Fract. Mech. **268**, 108444 (2022). https://doi.org/10.1016/j.engfracmech.2022.108444
72. Corral, E.L., Loehman, R.E.: Ultra-high-temperature ceramic coatings for oxidation protection of carbon–carbon composites. J. Am. Ceram. **91**, 1495–1502 (2008). https://doi.org/10.1111/j.1551-2916.2008.02331.x
73. Makurunje, P., Monteverde, F., Sigalas, I.: Self-generating oxidation protective high-temperature glass-ceramic coatings for Cf/C–SiC–TiC–TaC UHTC matrix composites. J. Eur. Ceram. **37**, 3227–3239 (2017). https://doi.org/10.1016/j.jeurceramsoc.2017.03.068
74. Wu, K., Zhou, Q., Cao, J., Qian, Z., Niu, B., Long, D.: Ultrahigh-strength carbon aerogels for high temperature thermal insulation. J. Colloid. Interface. Sci. **609**, 667–675 (2022). https://doi.org/10.1016/j.jcis.2021.11.067
75. Nagabandi, K., Pujari, A.K., Iyer, D.S.: Thermo-mechanical assessment of gas turbine combustor tile using locally varying thermal barrier coating thickness. Appl. Therm. Eng. **179**, 115657 (2020). https://doi.org/10.1016/j.applthermaleng.2020.115657
76. Zhao, K., Ye, F., Cheng, L., Zhou, J., Wei, Y., Cui, X.: Formation of ultra-high temperature ceramic hollow microspheres as promising lightweight thermal insulation materials via a molten salt-assisted template method. ACS Appl. Mater. Interfaces. **13**, 37388–37397 (2021). https://doi.org/10.1021/acsami.1c09662
77. Kumar, C.V., Kandasubramanian, B.: Advances in ablative composites of carbon based materials: a review. Ind. Eng. Chem. Res. **58**, 22663–22701 (2019). https://doi.org/10.1021/acs.iecr.9b04625
78. Gild, J., Zhang, Y., Harrington, T., Jiang, S., Hu, T., Quinn, M.C., Mellor, W.M., Zhou, N., Vecchio, K., Luo, J.: High-entropy metal diborides: a new class of high-entropy materials and a new type of ultrahigh temperature ceramics. Sci. Rep. **6**, 1–10 (2016). https://doi.org/10.1038/srep37946
79. Yan, X., Constantin, L., Lu, Y., Silvain, J.F., Nastasi, M., Cui, B.: $(Hf_{0.2}Zr_{0.2}Ta_{0.2}Nb_{0.2}Ti_{0.2})C$ high-entropy ceramics with low thermal conductivity. J. Am. Ceram. **101**, 4486–4491 (2018). https://doi.org/10.1111/jace.15779
80. Wei, X.F., Liu, J.X., Bao, W., Qin, Y., Li, F., Liang, Y., Xu, F., Zhang, G.J.: High-entropy carbide ceramics with refined microstructure and enhanced thermal conductivity by the addition of graphite. J. Eur. Ceram. **41**, 4747–4754 (2021). https://doi.org/10.1016/j.jeurceramsoc.2021.03.053
81. Backman, L., Gild, J., Luo, J., Opila, E.J.: Part I: theoretical predictions of preferential oxidation in refractory high entropy materials. Acta Mater. **197**, 20–27 (2020). https://doi.org/10.1016/j.actamat.2020.07.003
82. Castle, E., Csanádi, T., Grasso, S., Dusza, J., Reece, M.: Processing and properties of high-entropy ultra-high temperature carbides. Sci. Rep. **8**, 8609 (2018). https://doi.org/10.1038/s41598-018-26827-1